

Mechanism behind self-sustained oscillations in direct current glow discharges and in dusty plasmas

Sung Nae Cho*

Devices R&D Center, Samsung Advanced Institute of Technology,
Samsung Electronics Co., Ltd, Mt. 14-1 Nongseo-dong,
Giheung-gu, Yongin-si, Gyeonggi-do 446-712, Republic of Korea.

(Dated: 26 February 2013)

An alternative explanation to the mechanism behind self-sustained oscillations of ions in direct current (DC) glow discharges is provided. Such description is distinguished from the one provided by fluid models, where oscillations are attributed to positive feedback mechanism associated with photoionization of particles and photoemission of electrons from the cathode. Here, oscillations arise as consequence of interaction between an ion and surface charges induced by it at the bounding electrodes. Such mechanism provides an elegant explanation to why self-sustained oscillations occur only in the negative resistance region of the voltage-current characteristic curve in DC glow discharges. It is found that oscillation frequencies increase with ion's surface charge density, but at the rate which is significantly slower than it does with electric field. The presented mechanism also describes the self-sustained oscillations of ions in dusty plasmas, demonstrating that oscillations in dusty plasmas and DC glow discharges involve common physical processes.

I. INTRODUCTION

When an ion is confined between the two plane-parallel electrodes and is subject to a static electric field (see Fig. 1), it begins to self-oscillate without damping. Such phenomenon is referred to as self-sustained oscillations in direct current (DC) glow discharges; and, it has been known for almost a century.¹⁻⁷ In the literature, the DC glow discharges are also referred to as the DC glow corona. The mechanism behind such oscillations is still not fully understood.^{8,9,11-17} Over the years, various theoretical models have been proposed in an attempt to explain the phenomenon.^{5,11,18-26} Among the successful ones are those based on the fluid and equivalent circuit models.

The equivalent circuit models try to predict oscillations by representing the system with an equivalent RLC circuit, where R is resistor, L is inductor, and C is capacitor.¹⁸⁻²¹ Although this approach is quite useful in describing oscillation frequencies as function of DC bias voltages, it says nothing about the mechanism behind self-sustained oscillations.

The fluid models approach the problem from more fundamental grounds of the electromagnetic theory. In this approach, the Poisson equation is solved in combination with the electron and the ion flux continuity equations, which constitute the so called positive feedback mechanism.²²⁻²⁶ Assertion of such feedback mechanism is crucial in the fluid models because, without it, no oscillatory solutions can be obtained. Typical sources of positive feedback mechanism include the photoionization of particles and photoemission of electrons from the cathode. Physically, such feedback mechanism promotes oscillations by periodically reversing the particle's charge polarity. An ion oscillating near an electrode induces current in the same electrode, where the waveform of such current is correlated to its velocity profile.²³ Experimentally, it is this induced electrode current (or voltage) which gets measured.^{6,11} The hallmark of fluid models is their potential to reproduce experimental measurements to a reasonably good accuracy. In principle, with an appropriate specification of the positive feedback mechanism, the level of accuracy pre-

sented by fluid models can always be improved. The feedback mechanism varies among different authors, which has been a subject area of ongoing debate among different fluid model theorists.^{11,22-26}

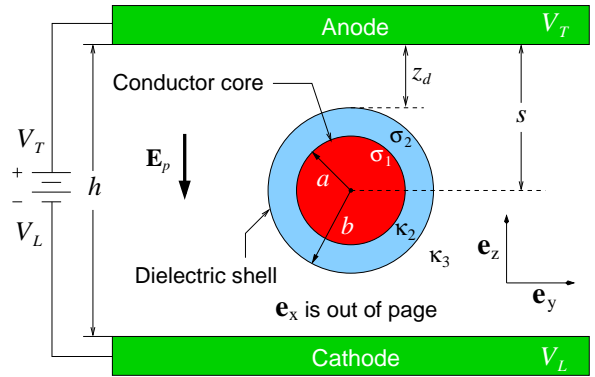


Figure 1: (Color online) Illustration of core-shell structured ion confined between DC voltage biased plane-parallel conductors with a vacuum gap of h . $\mathbf{E}_p = -\mathbf{e}_z(V_T - V_L)/h$ is the parallel plate electric field, where $(\mathbf{e}_x, \mathbf{e}_y, \mathbf{e}_z)$ are versors along the Cartesian (x, y, z) axes, respectively.

Does aforementioned positive feedback mechanism in fluid models represent the fundamental mechanism behind self-sustained oscillations in DC glow discharges? This is a subtle question because it has been shown recently that an ion confined between DC voltage biased plane-parallel conductors self-oscillates; and, such phenomenon only requires that an ion is electrically polarizable.²⁷ This excludes electrons from consideration, but a proton must self-oscillate in DC glow discharges as it is known to be electrically polarizable.²⁸ Remarkably, predictions of this alternative theory²⁹ qualitatively agree with predictions made by fluid models.^{23,25} Both predicts saw-tooth shaped waveforms for the induced electrode currents. Further, sharp pulses of radiation output are predicted by both theories to accompany the abrupt rises in the induced electrode currents. Such remarkable similarities

in the predictions by two dissimilar theories suggest that the positive feedback mechanism asserted in fluid models may not necessarily represent the fundamental mechanism behind the self-sustained oscillations in DC glow discharges.

In this work, I shall present new aspects of this alternative theory²⁹ for further exploitation of the self-sustained oscillations phenomenon in DC glow discharges. These theoretical predictions are explicitly compared with various experimental results for a validation of the model. By a direct application of the model to the charged-particle oscillations in a dusty (or complex) plasmas experiment, I shall reveal that self-sustained oscillations in both dusty plasmas and DC glow discharges involve a common physical mechanism, in which the particle oscillations are attributed to the interaction between an ionized particle and the surface charges induced by it at the surfaces of particle confining electrodes. Considering that particle oscillations in both dusty plasmas and DC glow discharges experiments involve ionized particles that are only differ by their physical sizes and masses, such outcome is not too surprising. After all, apart from this, everything else is nearly identical from the physics point of view in both experiments.

II. BRIEF OUTLINE OF THE THEORY

The self-sustained oscillations in DC glow discharges are now discussed briefly in the framework of presented alternative theory using the configuration in Fig. 1. The electric potential between the plates is obtained by solving the Laplace equation with appropriate boundary conditions.²⁷ With this electric potential, induced surface charges at the conductor plates are obtained by application of Gauss's law. Such charge distributions act on the ion and generate resultant force $\mathbf{F}_T = \mathbf{F}_1 + \mathbf{F}_2 - \mathbf{e}_z mg$, where m is ion's mass, $g = 9.8 \text{ m/s}^2$ is gravitational constant, and \mathbf{F}_1 (\mathbf{F}_2) is force between the ion and surface charges induced by the ion at the anode (cathode). The explicit forms of \mathbf{F}_1 and \mathbf{F}_2 are given by²⁷

$$\mathbf{F}_1 = \mathbf{e}_z \pi \epsilon_0 \kappa_3 v \left\{ \frac{v}{4s^2} + \left[\frac{\gamma(b^3 - a^3) - b^3}{4s^3} - 1 \right] E_p \right\},$$

$$\mathbf{F}_2 = \mathbf{e}_z \pi \epsilon_0 \kappa_3 v \left\{ \left[\frac{\gamma(b^3 - a^3) - b^3}{4(h-s)^3} - 1 \right] E_p - \frac{v}{4(h-s)^2} \right\},$$

where ϵ_0 is vacuum permittivity, $E_p \equiv \|\mathbf{E}_p\|$ is parallel-plate electric field strength, s is distance from ion's center to the anode; γ and v are given by

$$\gamma = \frac{3\kappa_3 b^3}{(\kappa_2 + 2\kappa_3)b^3 + 2(\kappa_2 - \kappa_3)a^3}, \quad (1)$$

$$v = \frac{2a(b-a)\sigma_1}{\epsilon_0 \kappa_2} + \frac{a^2 \sigma_1 + b^2 \sigma_2}{\epsilon_0 \kappa_3}, \quad (2)$$

where σ_1 (σ_2) is surface charge density at the ion's core (shell) of radius $r = a$ ($r = b$), and dielectric constants κ_2 and κ_3 are

depicted in Fig. 1. The resultant force on an ion is, hence,

$$\mathbf{F}_T(z_d) = \mathbf{e}_z \frac{\pi \epsilon_0 \kappa_3 v}{4} \left\{ \frac{v}{(z_d + b)^2} - \frac{v}{(h - z_d - b)^2} + \left[\frac{\gamma(b^3 - a^3) - b^3}{(z_d + b)^3} + \frac{\gamma(b^3 - a^3) - b^3}{(h - z_d - b)^3} - 8 \right] E_p \right\} - \mathbf{e}_z mg, \quad (3)$$

where $s = z_d + b$ in \mathbf{F}_1 and \mathbf{F}_2 (see Fig. 1). The associated potential energy is

$$U(z_d) = \frac{\pi \epsilon_0 \kappa_3 v}{4} \left\{ \frac{v}{z_d + b} + \frac{v}{h - z_d - b} - \frac{4v}{h} + \left[\frac{\gamma(b^3 - a^3) - b^3}{2(z_d + b)^2} - \frac{\gamma(b^3 - a^3) - b^3}{2(h - z_d - b)^2} + 8 \left(z_d + b - \frac{h}{2} \right) \right] E_p \right\} + mg \left(z_d + b - \frac{h}{2} \right); \quad (4)$$

and, the equation of motion for the force defined in Eq. (3) is given by

$$\frac{d^2 z_d}{dt^2} = \frac{\pi \epsilon_0 \kappa_3 v}{4m} \left\{ \frac{v}{(z_d + b)^2} - \frac{v}{(h - z_d - b)^2} + \left[\frac{\gamma(b^3 - a^3) - b^3}{(z_d + b)^3} + \frac{\gamma(b^3 - a^3) - b^3}{(h - z_d - b)^3} - 8 \right] E_p \right\} - g, \quad (5)$$

where γ and v are defined in Eqs. (1) and (2), respectively.^{27,29}

III. COMPARISON TO EXPERIMENTS

Gases under pressure in general, including noble gases, are composed of atomic clusters, a state of matter between molecules and solids, due to Van der Waals interaction.³⁰⁻³² In gaseous argon, each spherical atomic clusters of radius $r \approx 1 \text{ nm}$ contains roughly 135 argon atoms.³¹ Modeling particles in gas as atomic clusters is important because gases are delivered to the laboratories in a pressurized containers, in which environment individual gas particles exist in the state of atomic clusters. That said, I shall explicitly work with an argon atomic cluster of radius $r \approx 1 \text{ nm}$, which for brevity is referred to as "ion" hereafter. Such ion is not expected to be core-shell structured as illustrated in Fig. 1. The shell portion of an ion can be eliminated by choosing $b = a$, $\kappa_2 = \infty$, and $\sigma_2 = 0 \text{ C/m}^2$. For a positive ion, its surface charge density is given by $\sigma_1 = Nq_e / (4\pi a^2)$, where N is the number of electrons removed from the particle and $q_e = 1.602 \times 10^{-19} \text{ C}$ is the fundamental charge magnitude. Without loss of generality, and for the purpose of clear illustration in this work, I shall choose $N = 250$ and $a = 1 \text{ nm}$. This corresponds to ion's surface charge density of $\sigma_1 \approx 3.19 \text{ C/m}^2$. Assuming the mass of an argon atom is $6.63 \times 10^{-26} \text{ kg}$, cluster of 135 argon atoms has a total mass of $m \approx 8.95 \times 10^{-24} \text{ kg}$, neglecting

the masses of missing N electrons. For convenience, the cathode is grounded and a vacuum gap of $h = 100\text{ nm}$ is assumed between the plates in Fig. 1. That said, the parameters are summarized here for reference:

$$\left\{ \begin{array}{l} \kappa_2 = \infty, \quad \kappa_3 = 1, \quad h = 100\text{ nm}, \quad V_L = 0\text{ V}, \\ \sigma_1 \approx 3.19\text{ C/m}^2, \quad \sigma_2 = 0\text{ C/m}^2, \\ m \approx 8.95 \times 10^{-24}\text{ kg}, \quad b = a = 1\text{ nm}. \end{array} \right. \quad (6)$$

Illustrated in Fig. 2 is the plot of potential energy well, where Eq. (4) has been plotted for $V_T = 100\text{ V}$ using the values for parameters defined in Eq. (6). For the positive (negative) ion, the potential energy well appears near the anode (cathode) at the presence of static electric field. The presence of such potential energy well elegantly explains the self-sustained oscillations of an ion in DC glow discharges. It is remarkable that the profile of this potential energy well qualitatively agrees with the measurements by Tomme *et al.*³³ and Arnas *et al.*³⁴ in dusty plasmas. Further discussion on this is provided in sections A thru C of the appendix. The width of the potential energy well, i.e., l_D , decreases with increasing E_p . This explains why oscillation frequencies increase with the electric field strength. Fox seems to be the first to discuss on such characteristic using the parabolic potential model.³

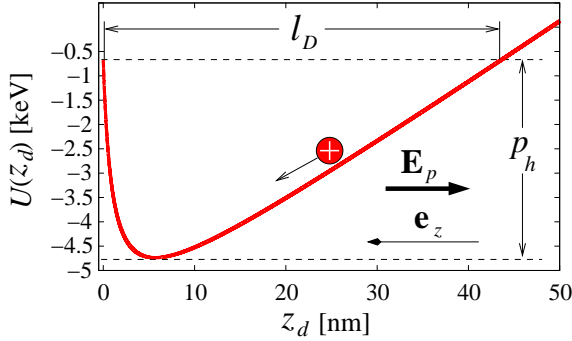


Figure 2: Potential energy is plotted for $V_T = 100\text{ V}$ using parameter values defined in Eq. (6). Here, $V_T = 100\text{ V}$ corresponds to $E_p = 1\text{ GV/m}$.

The particle's equation of motion, Eq. (5), has been solved via Runge-Kutta method using parameter values of Eq. (6) and the initial conditions given by

$$z_d(0) = 0.5\text{ nm} \quad \text{and} \quad \frac{dz_d(0)}{dt} = 0 \frac{\text{nm}}{\text{s}}. \quad (7)$$

The results for $V_T = 50\text{ V}$, 75 V , and 100 V are shown in Fig. 3(a), where it shows that oscillation frequencies are increasing with electric field strength. Oscillation frequencies also increase with ion's surface charge density, but at the rate which is significantly slower than it does with electric field, Fig. 3(b). For instance, when electric field strength is doubled from $E_p = 0.5\text{ GV/m}$ to $E_p = 1\text{ GV/m}$, oscillation frequency nearly doubles from $\nu_{\text{osc}} \approx 104\text{ GHz}$ to $\nu_{\text{osc}} \approx 191\text{ GHz}$. However, doubling ion's surface charge density, i.e., $\sigma_1 = Nq_e / (4\pi a^2)$, from $N = 250$ to $N = 500$ only slightly increases oscillation

frequency from $\nu_{\text{osc}} \approx 191\text{ GHz}$ to $\nu_{\text{osc}} \approx 207\text{ GHz}$. Such characteristics is consistent with observations by Fox³ and Bořan *et al.*,³⁵ where they reported oscillation frequencies do not seem to be very dependent on the type of ions used in the discharge. It is well known that dissimilar atomic gases have different ionization tendencies; and, it can be inferred that σ_1 for different atoms under identical conditions are generally different.

Although relatively high static electric field is applied to the ion in Fig. 3(a), its kinetic energies are small due to the frequent turnings occurring inside the tightly bound potential space. The ion's kinetic energy decreases with increased electric field strength for that matter, Fig. 3(c). At the maximum speed of $\sim 2.912\text{ km/s}$, the ion gains kinetic energy of $\mathcal{E}_K \approx 237\text{ eV}$, which is small compared to the depth of $p_h \approx 4.1\text{ keV}$ for the potential energy well, but large compared to the average room temperature thermal energy of $\mathcal{E}_T = 1.5k_B T \approx 39\text{ meV}$, where $T = 300\text{ K}$ and $k_B = 8.62 \times 10^{-5}\text{ eV/K}$ is the Boltzmann constant. The self-sustained oscillations in DC glow discharges can thus be expected to have high thermal stability.

In experiments, the self-sustained oscillations of ions in DC glow discharges occur only in the negative resistance region of the voltage-current characteristic curve.^{12,14,18,24} Such negative resistance region in the voltage-current characteristic curve is characterized by $V_{\text{th1}} \leq V_T \leq V_{\text{th2}}$, where V_{th1} and V_{th2} are some threshold voltages. Equation (5) provides an elegant explanation to such properties. For instance, Eq. (5) yields solutions that are unphysical for $E_p < E_{p,\text{th1}}$ and $E_p > E_{p,\text{th2}}$, where $E_{p,\text{th1}}$ and $E_{p,\text{th2}}$ are threshold electric field strengths. The physical solutions are only obtained for $E_{p,\text{th1}} \leq E_p \leq E_{p,\text{th2}}$. It is difficult to pinpoint $E_{p,\text{th1}}$ and $E_{p,\text{th2}}$ without the analytical solution of Eq. (5). Nevertheless, these can be roughly estimated on the grounds of physicality. To illustrate this, the oscillation frequency is first plotted as function of electric field strength in Fig. 3(d) by numerically solving Eq. (5) using parameter values and initial conditions from Eqs. (6) and (7), respectively. The solutions obtained for $E_p \lesssim 0.1\text{ GV/m}$ and $E_p \gtrsim 4.9\text{ GV/m}$ are unphysical. For instance, in the case of $E_p \gtrsim 4.9\text{ GV/m}$, solutions show the ion penetrating into the anode's surface whereas for $E_p \lesssim 0.1\text{ GV/m}$, solutions yield peak to peak amplitudes that are larger than $h/2$. This latter case is unphysical because, for a positive ion, oscillations can only exist for $z_d < h/2 - b$.²⁷ The physical oscillatory solutions exist only for $0.1\text{ GV/m} \lesssim E_p \lesssim 4.9\text{ GV/m}$, where the upper and lower bounds of E_p are rough estimates based on the grounds of discussed physicality. Further discussion on the properties of physical and unphysical oscillatory solutions are provided in section D of the appendix.

Recently, Lotze *et al.*³⁶ reported on an indirect account of oscillations involving single H_2 molecule in DC voltage biased conductors near absolute zero temperature of $T = 5\text{ K}$. According to their finding, the H_2 molecule in the junction, a space between atomically clean Cu(111) surface and the STM (scanning tunneling microscope) tip mounted on a cantilever, self-oscillates between the two unknown positional states when threshold DC bias voltage is applied to the elec-

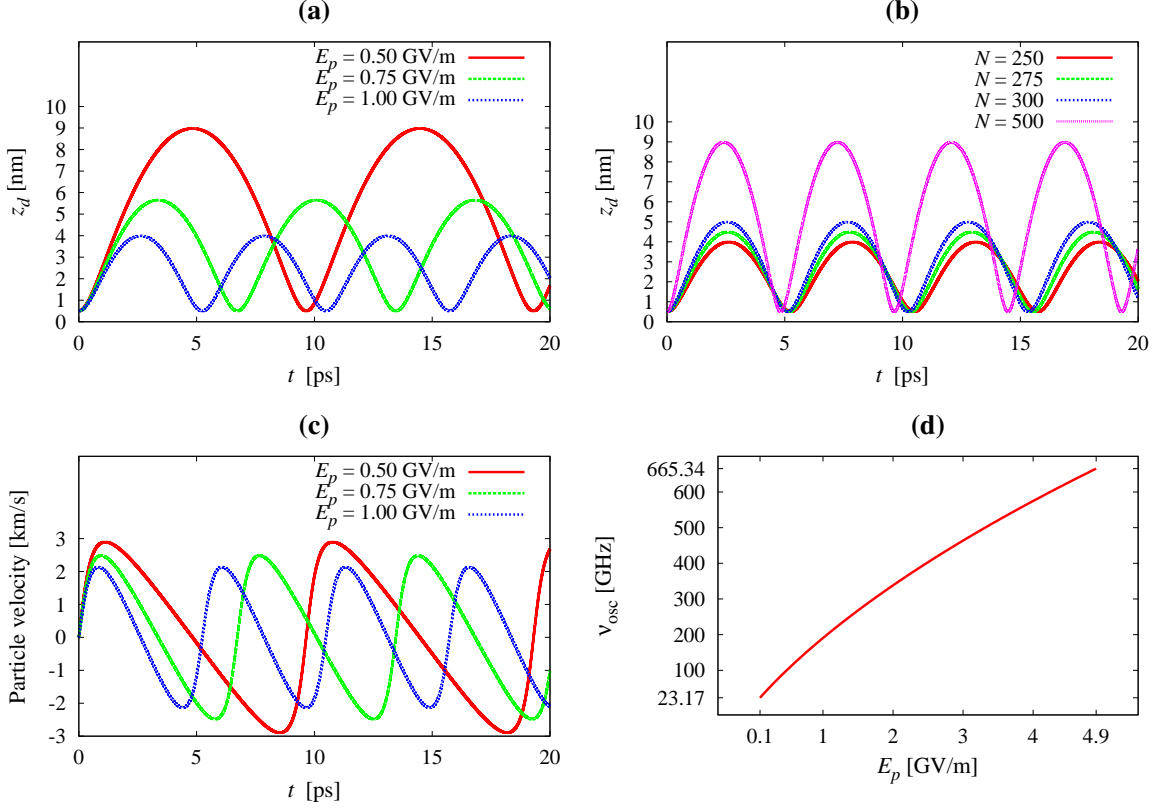


Figure 3: (Color online) Equation (5) is plotted, where in (a) electric field is varied and in (b) ion's surface charge density $\sigma_1 = Nq_e / (4\pi a^2)$ is varied at $E_p = 1 \text{ GV/m}$. (c) Ion velocity corresponding to the plot in (a). (d) Dependence of oscillation frequency v_{osc} on electric field strength E_p . Similar plot for the lower frequencies involving weakly charged ions subject to smaller E_p is also provided in the section E of appendix. In (a,b,c,d), all of the unspecified parameter values are from Eq. (6) and the initial conditions are from Eq. (7).

trodes, i.e., the copper Cu (111) surface and the STM tip. The footprint of self-sustained oscillations is the presence of negative differential conductance in their measurement. Gupta *et al.*³⁷ showed that such negative differential conductance is due to H_2 molecules in the junction. In DC glow discharges, self-sustained oscillations arise as consequence of negative differential resistance.^{10,12,14} Since negative differential conductance and negative differential resistance are reciprocally related, they represent equivalent descriptions of the same physical processes. It is well known that H_2 molecules are ionized by electron impact.³⁸ When threshold DC bias voltage is applied to the electrodes, energetic electrons begin to tunnel through the junction. It is possible that H_2 molecules in the junction are ionized in the process. If that is indeed the case, what Lotze *et al.* reported may be an indirect account of self-sustained oscillations involving single or few ions in DC glow corona.²⁹ Their observation can serve as catalyst for future experiments in few-particle DC plasmas.

Arnas *et al.*³⁹ reported that a dust particle made of hollow glass microsphere of radius $r \approx 32 \mu\text{m}$ with mass density of $\rho_m \approx 110 \text{ kg/m}^3$ and carrying a total electrical charge of $Q \approx -4.3 \times 10^5 q_e$, where $q_e = 1.602 \times 10^{-19} \text{ C}$, self-oscillates at a frequency of $v_{\text{osc}} \approx 17 \text{ Hz}$ inside the plasma sheath. The plasma sheath environment, in many respects, is similar to

an empty space region between the DC voltage biased plane-parallel conductors. Ionized particle oscillations in the plasma sheath can therefore be modeled from the simple apparatus illustrated in Fig. 1. That explained, the parameters and initial conditions in the experiment by Arnas *et al.* can be summarized as

$$\begin{cases} \kappa_2 = 6.5, \quad \kappa_3 = 1, \quad h = 5 \text{ mm}, \quad E_p = 5.15 \text{ kV/m}, \\ \sigma_1 = 0 \text{ C/m}^2, \quad \sigma_2 = -5.35 \mu\text{C/m}^2, \\ m \approx 15.1 \text{ ng}, \quad a = 0 \text{ m}, \quad b = 32 \mu\text{m}, \\ z_d(0) = 4.4 \text{ mm}, \quad \dot{z}_d(0) = 0 \text{ mm/s}, \quad \dot{z}_d \equiv dz_d/dt, \end{cases} \quad (8)$$

where the details of how these were obtained are explained in section B of the appendix. With these, the equation of motion described in Eq. (5) is solved numerically via Runge-Kutta method; and, the result is shown in Fig. 4, where it shows the particle oscillation frequency of approximately $v_{\text{osc}} \approx 17 \text{ Hz}$, consistent with the result obtained by Arnas *et al.*³⁹

Although Arnas *et al.* explicitly states that their glass microsphere is hollow structured, their paper does not provide any information regarding the radius of a void inside the hollow glass microsphere. Due to lack of this information, the mass of hollow glass microsphere in Eq. (8) has been computed assuming a solid microsphere, which overestimates the mass. In fact, their paper provides gravitational force of $F_g = (1.5 \pm 0.3) \times 10^{-10} \text{ N}$ for the glass microsphere.³⁹ Such

force corresponds to a mass of $m \approx 15.3$ ng, which is exactly the mass computed assuming a solid microsphere in Eq. (8). If instead a smaller mass of $m \approx 6.19$ ng is assumed, $E_p = 2.2$ kV/m is sufficient to generate oscillation frequency of $\nu_{\text{osc}} \approx 17$ Hz, where $E_p = 2.2$ kV/m is in the range of local electric field strengths (measured by Arnas *et al.*) in the plasma sheath. This result is plotted in Fig. 4 for a comparison with the case obtained for $m \approx 15.1$ ng and $E_p = 5.15$ kV/m.

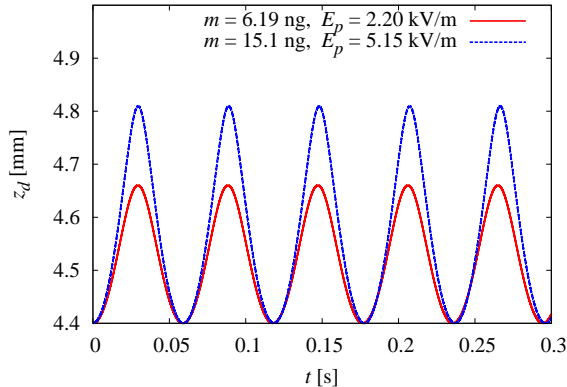


Figure 4: (Color online) Equation (5) is plotted using parameter values and initial conditions defined in Eqs. (8). Oscillation frequency of $\nu_{\text{osc}} \approx 17$ Hz is predicted by the theory, which is consistent with the measurement by Arnas *et al.*³⁹ In the plot, the anode is located at $z_d = 0$ mm and the cathode is located at $z_d = 5$ mm.

This remarkable result demonstrates that self-sustained oscillations in both dusty plasmas and DC glow discharges share a common physical mechanism, in which the oscillations are attributed to the interaction between the ionized particle and the surface charges induced by it at the bounding, DC voltage biased, electrodes. Such outcome makes sense because oscillating ionized particles in both dusty plasmas and DC glow discharges experiments are only differ in their physical sizes; and, with the exception of this, the two systems are nearly identical in nature.

Quite often in dusty plasmas, theoretical models based on simple harmonic excitations of small amplitude oscillations are employed for the description of the particle dynamics. One such model is given by⁴⁰

$$\frac{d^2z}{dt^2} + \nu_{\text{dn}} \frac{dz}{dt} + \Omega_v^2 z = \frac{f_0 \cos \omega t}{m_d}, \quad (9)$$

where z is the particle displacement, m_d is the particle's mass, ω is the angular frequency of oscillation, t is the time, and f_0 is the amplitude of external force. Particle's equation of motion based on such model, Eq. (9), is limited to descriptions of oscillations involving small amplitude displacements about the stationary equilibrium position. Besides this limitation, the equation of motion described in Eq. (9), as it stands, cannot be directly applied for the description of particle's oscillatory motion due to the fact that quantities ν_{dn} and Ω_v must be first determined experimentally.⁴¹ Consequently, Eq. (9) is only useful when determining the total charge carried by the

particle. Equation (9) provides an indirect method of measuring the particle's total charge; however, as it stands, it cannot be directly used to explain the fundamental mechanism behind self-sustained ion oscillations in dusty plasmas.

The equation of motion described in Eq. (5) is distinguished from the one illustrated in Eq. (9) in that its physical description is not limited to just small amplitude oscillations but covers particle oscillations of any amplitude ranges. Further, Eq. (5) does not depend on quantities like ν_{dn} and Ω_v , which terms must be determined experimentally. Instead, Eq. (5) completely describes the dynamics of charged-particle motion solely based on the information obtained from the particle's physical properties (i.e., mass, surface charge density, and dielectric constant, etc.) and the local electric field strength. In the case where the mass of an ionized particle is represented by that of an ionized atom, Eq. (5) describes the dynamics of self-oscillating ionized atom in DC glow discharges. In the previous work,²⁹ I have discussed that Eq. (5) yields results that qualitatively agree with certain aspects of self-oscillations in DC glow corona experiments predicted by theories based on the fluid models.^{23,25} If the plasma in DC glow corona experiment is effectively treated as a self-oscillating weakly ionized single *superparticle*, Eq. (5) provides a satisfactory description of the electrode current oscillations in DC glow corona. Further discussion on this is provided in section E of the appendix.

Until now, no single theory was able to successfully explain self-sustained oscillations in both dusty plasmas and DC glow discharges experiments. For years, experimental evidences hinted that these were related phenomena, but without any definitive conclusions. In this respect, Eq. (5) is the first theoretical model to provide such definitive conclusions.

IV. DEVICE APPLICATION

Oscillating ions generate electric dipole radiation,^{27,29} which property can be utilized to develop wideband electromagnetic radiation sources. In such device, frequency is tuned by varying the DC bias voltage across the electrodes. According to Zouche and Lefort, plate electrodes separated by a gap of $h = 100$ nm and made of nickel-silver composite material can support DC voltages up to ~ 400 V before an onset of electrical breakdown.⁴² With improvements in electrical breakdown characteristics, such device can be engineered to cover both microwave and terahertz band of frequencies.

V. CONCLUDING REMARKS

In summary, the mechanism behind self-sustained oscillations of an ion in DC glow discharges has been briefly discussed in the framework of interaction between an ion and surface charges that it induces at the bounding electrodes. It has been found that oscillation frequencies also increase with ion's surface charge density, but at the rate which is significantly slower than it does with electric field strength. Such result supports the conclusions by Fox³ and Bořan *et al.*,³⁵

where they reported of oscillation frequencies being not too dependent on the type of ions used in the discharge. Self-sustained oscillations in DC glow discharges can be expected to have high thermal stability due to ion's kinetic energies that are much larger than the average room temperature thermal energies. It is well known that self-sustained oscillations in DC glow discharges occur only in the negative resistance region of the voltage-current characteristic curve. Experimentally, such region is characterized by $V_{th1} \leq V_T \leq V_{th2}$, where V_{th1} and V_{th2} are some threshold voltages. Such observation is quite elegantly explained from the solutions of Eq. (5), where the physical solutions are only found for $V_{th1} \leq V_T \leq V_{th2}$. Presented mechanism also correctly describes the self-sustained oscillations of ions in dusty plasmas. To demonstrate this, Eq. (5) has been applied to correctly predict the frequency of dust particle oscillations in the dusty plasmas experiment by Arnas *et al.*³⁹ Such result demonstrates that self-sustained oscillations in dusty plasmas and DC glow discharges involve common physical processes. This is the first theory to successfully explain the self-sustained oscillations phenomena in both dusty plasmas and the DC glow corona physics.

APPENDIX

A. Sheath potential

It is worthwhile to compare the potential energy well of Fig. 2 with the empirical potential well introduced by Tomme *et al.*³³ to describe the potential in the plasma sheath. The plasma sheath is an empty space residing between the plasma and the confining electrodes. One such plasma sheath near the anode is illustrated in Fig. 5(a). For the reason that electrons and ions move at different velocities due to the difference in their masses, plasmas are never completely neutral at any instant. Consequently, a plasma confined between DC voltage biased electrodes effectively behaves as if it were a super large charged-particle. For brevity, such “super large charged-particle” shall be simply referred to as a “plasma ball” throughout the discussion here. In fact, the single ionized nanoparticle case illustrated in Fig. 5(b) is the limit in which the plasma in Fig. 5(a) reduces down to contain just one ionized nanoparticle. That said, just as single ionized nanoparticle self-oscillates when confined by DC voltage biased electrodes, the plasma ball also self-oscillates between the anode and cathode electrodes.⁹ However, due to its large mass, the plasma ball oscillates at much lower frequencies compared to the nanoparticle counterparts. For instance, assuming the gap h between the plate electrodes is in the order of sub-millimeters or so in Fig. 5(a), the macroscopic plasma confined between such electrodes can contain very large number, i.e., say, millions or more, of ionized nanoparticles or atoms depending on the gas pressure. In general, for the study of self-sustained oscillations, the plasma ball illustrated in Fig. 5(a) can be effectively modeled using an ionized superparticle, where the terminology “superparticle” refers to a particle which is extremely large and enormously heavier compared to the ionized nanoparticle (or atom) illustrated in Fig. 5(b). In

such model, the potential in the plasma sheath is represented by the one presented in this article. It is quite remarkable that the sheath potential introduced empirically by Tomme *et al.* closely resembles the potential described in this work.

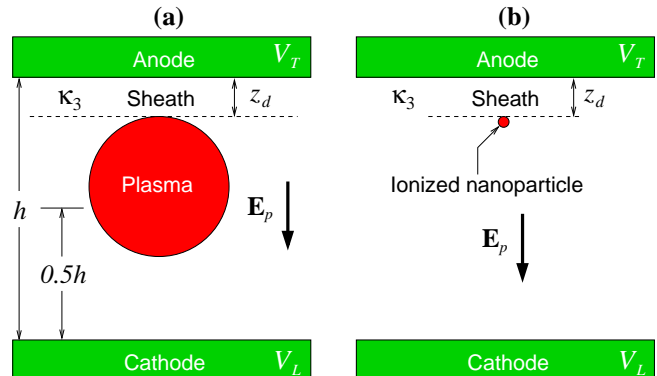


Figure 5: (Color online) (a) Illustration of the plasma and the sheath. The plasma ball effectively behaves as one very large charged superparticle. In the illustration, the plasma has been deliberately drawn as a sphere to emphasize a plasma ball. In reality, however, the plasma can be in any shape depending on the geometry of confining electrodes. (b) The single ionized particle configuration considered in this article. In (a) and (b), only the sheath near the anode is shown for illustration.

B. Parameters in experiment by Arnas *et al.*

Arnas *et al.*³⁹ reported that a dust particle made of hollow glass microsphere of radius $r \approx 32 \mu\text{m}$ with mass density $\rho_m \approx 110 \text{kg/m}^3$ and carrying a total charge of $Q \approx -4.3 \times 10^5 q_e$, where $q_e = 1.602 \times 10^{-19} \text{C}$, self-oscillates at frequency of $\nu_{osc} \approx 17 \text{Hz}$ inside the plasma sheath. The inner environment of the plasma sheath, in many respects, is similar to the environment in an empty space between the DC voltage biased plane-parallel conductors. In that regard, the undamped self-sustained oscillations of charged glass microsphere in the experiment by Arnas *et al.* should be theoretically describable using the model presented in this article, where a core-shell structured charged particle is confined between the DC voltage biased plane-parallel conductors. The glass microsphere used by Arnas *et al.* is not core-shell structured, of course. Such dielectric particle is obtained in the limit the radius of conductive core portion of the core-shell structured particle goes to zero, i.e., $a = 0$. Consequently, σ_1 also vanishes in that limit. That said, the glass microsphere of radius $b = 32 \mu\text{m}$ with mass density $\rho_m \approx 110 \text{kg/m}^3$ has total mass of $m = (4/3)\pi b^3 \rho_m$ or $m \approx 1.51 \times 10^{-11} \text{kg}$. Although Arnas *et al.* specifically uses the word “hollow glass microsphere” in their report, they do not provide any physical details of the particle other than its outer radius. Thus, in the aforementioned calculation of the particle's mass, I have assumed a solid glass microsphere. The glass microsphere carries a total charge of $Q \approx -4.3 \times 10^5 q_e$, where $q_e = 1.602 \times 10^{-19} \text{C}$. The surface charge density at the radius $r = b$ is hence given

by $\sigma_2 = Q/(4\pi b^2)$ or $\sigma_2 = -5.35 \mu\text{C}/\text{m}^2$. Arnas *et al.* does not provide any information regarding the dielectric constant κ_2 for their glass microsphere. Therefore, $\kappa_2 = 6.5$ has been chosen for the dielectric constant of glass microsphere, which value is typical of glass microspheres. For convenience, it shall be assumed that the medium in which the glass microsphere oscillates is a vacuum, i.e., $\kappa_3 = 1$. The parameters in the experiment by Arnas *et al.* is summarized here for reference:

$$\begin{cases} \kappa_2 = 6.5, \kappa_3 = 1, h = 5 \text{ mm}, E_p = 5.15 \text{ kV/m}, \\ \sigma_1 = 0 \text{ C/m}^2, \sigma_2 = -5.35 \mu\text{C}/\text{m}^2, \\ m \approx 15.1 \text{ ng}, a = 0 \text{ m}, b = 32 \mu\text{m}, \end{cases} \quad (10)$$

where the mass is in nanograms, i.e., $m \approx 1.51 \times 10^{-11} \text{ kg} = 15.1 \text{ ng}$. The initial conditions,

$$z_d(0) = 4.4 \text{ mm} \quad \text{and} \quad \frac{dz_d(0)}{dt} = 0 \frac{\text{mm}}{\text{s}}, \quad (11)$$

have been chosen purely out of convenience. With Eqs. (10) and (11), the equation of motion defined in Eq. (5) can be solved numerically via Runge-Kutta method to obtain the results illustrated in Fig. 4. One can readily verify that the theory agrees with the experiment.³⁹

C. Comparison to the potential energy of negatively charged glass microsphere measured by Arnas *et al.*

According to the model elaborated here,²⁹ the positively charged particle confined between a DC voltage biased plane-parallel conductors results in the formation of potential energy well in vicinity of the anode whereas a negatively charged particle results in the formation of potential energy well in vicinity of the cathode. Arnas *et al.*³⁴ have experimentally verified such potential energy well for the case of negatively charged particle in the plasma sheath near the cathode. As explained previously, the problem of charged particle inside the plasma sheath can be effectively modeled by a charged particle confined by the DC voltage biased plane-parallel conductors. The potential energy function $U(z_d)$ of Eq. (4) has been plotted for the following parameter values:

$$\begin{cases} \kappa_2 = 6.5, \kappa_3 = 1, h = 5 \text{ mm}, E_p = 3.15 \text{ kV/m}, \\ \sigma_1 = 0 \text{ C/m}^2, \sigma_2 = -5.795 \mu\text{C}/\text{m}^2, \\ m \approx 4.91 \times 10^{-12} \text{ kg}, a = 0 \text{ m}, b = 22 \mu\text{m}. \end{cases} \quad (12)$$

The result is shown in Fig. 6, where it shows the formation of potential energy well in vicinity of the cathode. One notices that the order of magnitude for the potential energy well is comparable to the experiment by Arnas *et al.* The minor discrepancies in the potential energy well of Fig. 6 and the one measured by Arnas *et al.*³⁴ can be attributed to the fact that the electric field is not constant in the plasma sheath whereas, between the DC voltage biased plane-parallel conductors, electric field is a constant.

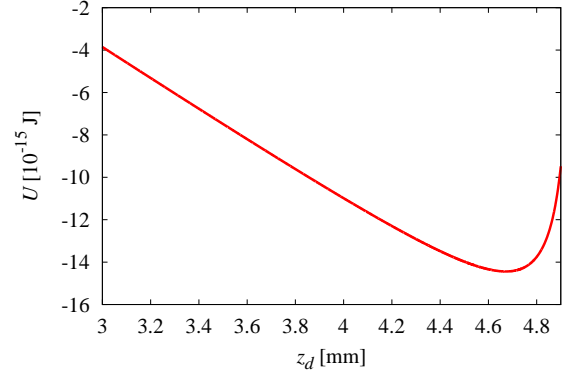


Figure 6: The potential energy of Eq. (4) is plotted for parameter values defined in Eq. (12). In the plot, the anode is located at $z_d = 0 \text{ mm}$ and the cathode is located at $z_d = 5 \text{ mm}$. This result should be compared with the potential energy measured by Arnas *et al.*³⁴ in their dusty plasmas experiment. One can verify that two results are remarkably similar in potential energy profile as well as in the order of magnitudes.

D. Physical and unphysical oscillatory solutions

The oscillatory solutions obtained for $E_p \lesssim 0.1 \text{ GV/m}$ and $E_p \gtrsim 4.9 \text{ GV/m}$ are unphysical in Fig. 3(d). To demonstrate this, Eq. (5) is numerically solved and plotted for $E_p \lesssim 0.1 \text{ GV/m}$ and $E_p \gtrsim 4.9 \text{ GV/m}$ using the following initial conditions and parameter values:

$$\begin{cases} \kappa_2 = \infty, \kappa_3 = 1, h = 100 \text{ nm}, V_L = 0 \text{ V}, \\ \sigma_1 \approx 3.19 \text{ C/m}^2, \sigma_2 = 0 \text{ C/m}^2, \\ m \approx 8.95 \times 10^{-24} \text{ kg}, b = a = 1 \text{ nm}, \\ z_d(0) = 0.5 \text{ nm}, \dot{z}_d(0) = 0 \text{ nm/s}, \dot{z}_d \equiv dz_d/dt. \end{cases} \quad (13)$$

To show that $E_p \lesssim 0.1 \text{ GV/m}$ yields unphysical solutions, $z_d(t)$ is plotted for $E_p = 0.1 \text{ GV/m}$ and $E_p = 0.09 \text{ GV/m}$. The results are shown in Fig. 7, where the surface of anode is at $z_d = 0 \text{ nm}$, the surface of cathode is at $z_d = 100 \text{ nm}$, and the midway between the plates is at $z_d = 50 \text{ nm}$. It can be clearly seen that for $E_p = 0.09 \text{ GV/m}$, positively ionized particle periodically crosses the midway between the two electrodes. Such case is unphysical because, for positively ionized particles, oscillations can only exist for $z_d < h/2 - b$.²⁷ Now, it can be verified that any E_p less than $E_p = 0.09 \text{ GV/m}$ yields such unphysical solutions.

To show that $E_p \gtrsim 4.9 \text{ GV/m}$ yields unphysical solutions, $z_d(t)$ is plotted for $E_p = 4.9 \text{ GV/m}$ and $E_p = 5.0 \text{ GV/m}$. The results are shown in Fig. 8(a), where the plot has been enlarged for a view near $z_d = 0 \text{ pm}$ in Fig. 8(b). It can be clearly seen that for $E_p = 5.0 \text{ GV/m}$, positively ionized particle periodically penetrates into the surface of anode, which is unphysical. Now, it can be verified that any E_p larger than $E_p = 5.0 \text{ GV/m}$ yields such unphysical solutions.

For the initial conditions and parameter values defined in Eq. (13), physical solutions for the oscillatory motion of positively ionized particle are only found for E_p satisfying the condition given by $0.1 \text{ GV/m} \lesssim E_p \lesssim 4.9 \text{ GV/m}$, where the

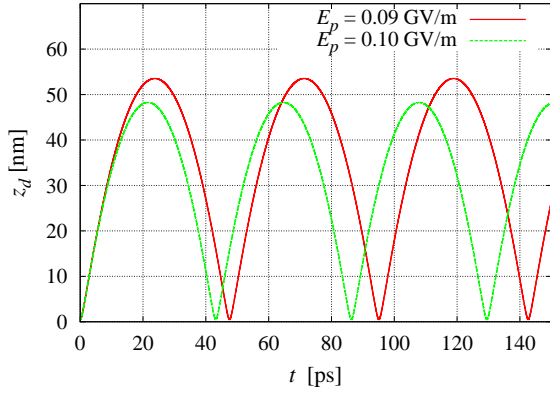


Figure 7: (Color online) Plot of $z_d(t)$ for $E_p = 0.1$ GV/m and $E_p = 0.09$ GV/m. The surface of anode is at $z_d = 0$ nm, the surface of cathode is at $z_d = 100$ nm, and the midway between the two electrodes is at $z_d = 50$ nm.

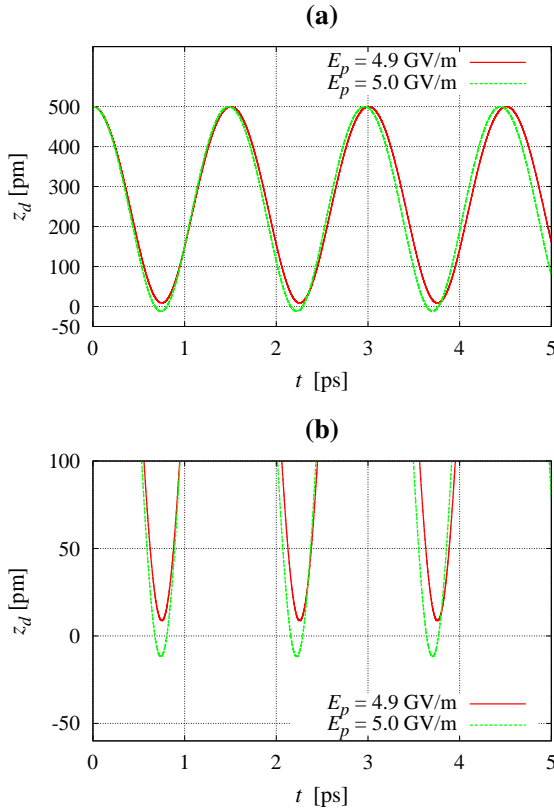


Figure 8: (Color online) (a) Plot of $z_d(t)$ for $E_p = 4.9$ GV/m and $E_p = 5.0$ GV/m. (b) The plot in (a) has been enlarged for a view near $z_d = 0$ pm. The surface of anode is at $z_d = 0$ pm.

upper and lower bounds of E_p are rough estimates based on the grounds of the discussed physicality. This result explains why oscillations suddenly appear at certain “initial” threshold DC bias voltage and disappear suddenly when bias voltage goes beyond certain larger “final” threshold voltage in experiments.

E. Weakly ionized particle confined between anode and cathode plates separated by gap of $h = 1$ mm

The oscillation frequency plot of Fig. 3(d) has been obtained for an highly ionized particle which is confined between two plate electrodes with very small separation gap of $h = 100$ nm. Here, the same calculation is done for a weakly ionized particle confined between plate electrodes with microscopically very large separation gap of $h = 1$ mm. According to Chen *et al.*,³² a spherical argon cluster of radius $r = a = 4.7$ nm contains roughly ~ 9600 argon atoms at backing pressure of 50 bars. Since the particle is assumed to be weakly ionized, I shall assume that $N = 20$ electrons are removed from it. This corresponds to surface charge density of $\sigma_1 = Nq_e / (4\pi a^2)$ or $\sigma_1 \approx 1.1543 \times 10^{-2} \text{ C/m}^2$, where $q_e = 1.602 \times 10^{-19} \text{ C}$ is the fundamental charge unit. Neglecting the masses of missing N electrons, the particle has a total mass of $m \approx 6.365 \times 10^{-22} \text{ kg}$. For the calculation of particle’s mass, it has been assumed that single argon atom has mass of $6.63 \times 10^{-26} \text{ kg}$. That said, the following initial conditions and parameter values are used for the calculation of particle’s oscillation frequency as function of electric field strength:

$$\begin{cases} \kappa_2 = \infty, \kappa_3 = 1, h = 1 \text{ mm}, V_L = 0 \text{ V}, \\ \sigma_1 \approx 11.543 \text{ mC/m}^2, \sigma_2 = 0 \text{ C/m}^2, \\ m \approx 6.365 \times 10^{-22} \text{ kg}, b = a = 4.7 \text{ nm}, \\ z_d(0) = 10 \mu\text{m}, \dot{z}_d(0) = 0 \mu\text{m/s}, \dot{z}_d \equiv dz_d/dt. \end{cases} \quad (14)$$

Using these, the equation of motion defined in Eq. (5) is solved numerically via Runge-Kutta method for the oscillation frequency as function of electric field strength; and, the result is shown in Fig. 9.

This result should be compared with the one provided by Akishev *et al.*,²⁵ where they have plotted both experimental and calculated period T_{osc} of self-sustained oscillations against the average corona current at different pressures of nitrogen. Fox³ and Bořan *et al.*³⁵ have shown that oscillation frequencies are not very dependent on the type of ionized particles used in the discharge. That said, the result obtained by Akishev *et al.* for nitrogen gas can be compared with the calculation done here for ionized spherical argon cluster. Recalling that $\nu_{\text{osc}} = 1/T_{\text{osc}}$ and the average corona current in the electrode increases with electric field strength, it can be readily convinced that the profile of result shown in Fig. 9 is consistent with the result obtained by Akishev *et al.*

Although the profile of oscillation frequency dependence on electric field strength (or corona current in the electrode) is comparable in both results, the measurement by Akishev *et al.* shows much lower oscillation frequencies for given range of electric field strengths. Why? Such discrepancy arises from the fact that in the experiment by Akishev *et al.*, the self-oscillating object is a charged plasma ball, i.e., charged superparticle, whereas in the calculation of Fig. 9, the self-oscillating object is a charged nanoparticle. As already discussed in section A, a macroscopic plasma ball contains very large number of ionized nanoparticles (or atoms) depending on the gas pressure. This makes macroscopic plasma ball effectively a single charged-superparticle with very large mass.

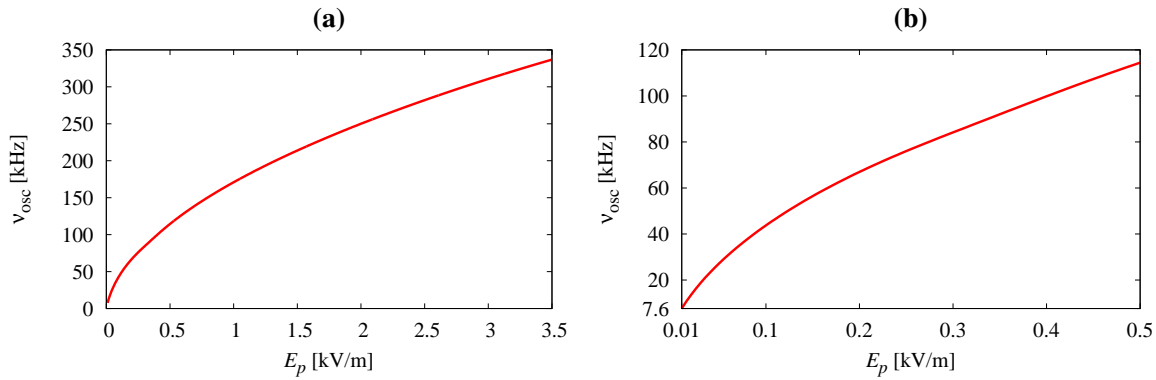


Figure 9: (a) The frequency of oscillations is plotted against electric field strength for a weakly ionized particle with initial conditions and parameters values defined in Eq. (14). (b) The plot in (a) is enlarged near zero. Unlike the case illustrated in Fig. 3(d), where ionized particle is confined between electrodes with very small gap, the result here involves very large number of discretized time steps for the Runge-Kutta routine. For that reason, the oscillation frequency has been plotted from $E_p = 0.01$ kV/m to $E_p = 3.5$ kV/m in (a). The threshold electric field strengths, i.e., $E_{p,th1}$ and $E_{p,th2}$, are not shown in the figure.

It has been illustrated in Fig. 4 that an ionized particle with smaller mass requires weaker electric field strength compared to the one with larger mass to oscillate at the same frequency. Mathematically, such characteristic arises from the fact that Eq. (5) has mass dependence in the denominator. Consequently, the plasma ball in the experiment by Akishev *et al.*, which effectively behaves as a single charged-superparticle, oscillates at much lower frequencies for the given range of

electric field strengths compared to the configuration used in Fig. 9, where the mass of an ionized particle is much smaller than the effective mass of a plasma ball. In principle, once the mass and the effective total charge information of the plasma ball, i.e., superparticle, are provided, the oscillation frequency dependence on corona current in the electrode (or electric field strength) measured by Akishev *et al.* can be reproduced by the presented theory.

-
- * Electronic address: sungnae.cho@samsung.com
- ¹ L. Pardue and J. Webb, Phys. Rev. **32**, 946 (1928).
 - ² G. Fox, Phys. Rev. **35**, 1066 (1930).
 - ³ G. Fox, Phys. Rev. **37**, 815 (1931).
 - ⁴ T. Donahue and G. Dieke, Phys. Rev. **81**, 248 (1951).
 - ⁵ L. Colli, U. Facchini, E. Gatti, and A. Persano, J. Appl. Phys. **25**, 429 (1954).
 - ⁶ A. Pilon, Phys. Rev. **107**, 25 (1957).
 - ⁷ K. Ogawa, J. Phys. Soc. Jpn. **14**, 1746-1751 (1959).
 - ⁸ M. Goldman, A. Goldman, and R. Sigmond, Pure & Appl. Chem. **57**(9), 1353-1362 (1985).
 - ⁹ A. Piel, H. Klostermann, A. Rohde, N. Jelić, and R. Schrittwieser, Phys. Lett. A **216**, 296 (1996).
 - ¹⁰ Z. Petrović, I. Stefanović, S. Vrhovac, and J. Živković, J. Phys. IV France **7**, C4-341 (1997).
 - ¹¹ R. Sigmond, J. Phys. IV France **7**, C4-383 (1997).
 - ¹² Z. Petrović and A. Phelps, Phys. Rev. E. **56**, 5920 (1997).
 - ¹³ K. Schoenbach, A. El-Habachi, W. Shi, and M. Ciocca, Plasma Sources Sci. Technol. **6**, 468 (1997).
 - ¹⁴ E. Lozneanu, V. Popescu, and M. Sanduloviciu, J. Appl. Phys. **92**, 1195 (2002).
 - ¹⁵ M. Makarov, Y. Loumani, and A. Kozyrev, J. Appl. Phys. **100**, 033301 (2006).
 - ¹⁶ R. Stenzel, J. Gruenwald, C. Ionita, and R. Schrittwieser, Plasma Sources Sci. Technol. **20**, 045017 (2011).
 - ¹⁷ T. Kuschel, B. Niermann, I. Stefanović, M. Böke, N. Škoro, D. Marić, Z. Petrović, and J. Winter, Plasma Sources Sci. Technol. **20**, 065001 (2011).
 - ¹⁸ A. Phelps, Z. Petrović, and B. Jelenković, Phys. Rev. E. **47**, 2825 (1993).
 - ¹⁹ D. Hsu and D. Graves, J. Phys. D: Appl. Phys. **36**, 2898 (2003).
 - ²⁰ P. Chabert, C. Lazzaroni, and A. Rousseau, J. Appl. Phys. **108**, 113307 (2010).
 - ²¹ S. He, J. Ouyang, F. He, and H. Jia, Phys. Plasmas **19**, 023504 (2012).
 - ²² I. Pérès and L. Pitchford, J. Appl. Phys. **78**, 774 (1995).
 - ²³ R. Morrow, J. Phys. D: Appl. Phys. **30**, 3099 (1997).
 - ²⁴ Z. Donkó, J. Phys. D: Appl. Phys. **32**, 1657 (1999).
 - ²⁵ Yu. Akishev, M. Grushin, A. Deryugin, A. Napartovich, M. Pan'kin, and N. Trushkin, J. Phys. D: Appl. Phys. **32**, 2399 (1999).
 - ²⁶ N. Allen, M. Abdel-Salam, M. Boutlendj, I. Cotton, and B. Tan, IET Sci. Meas. Technol. **1**(2), 103 (2007).
 - ²⁷ S. Cho, Phys. Plasmas **19**, 033506 (2012).
 - ²⁸ B. MacGibbon, G. Garino, M. Lucas, A. Nathan, G. Feldman, and B. Dolbilkin, Phys. Rev. C **52**, 2097 (1995).
 - ²⁹ S. Cho, Phys. Plasmas **19**, 072113 (2012).
 - ³⁰ E. Becker, K. Bier, and W. Henkes, Z. Phys. **146**, 133 (1956).
 - ³¹ L. Bartell, B. Raoult, and G. Torchet, J. Chem. Phys. **66**, 5387 (1977).
 - ³² G. Chen, B. Kim, B. Ahn, and D. Kim, J. Appl. Phys. **106**, 053507 (2009).
 - ³³ E. Tomme, B. Annaratone, and J. Allen, Plasma Sources Sci. Technol. **9**, 87 (2000).
 - ³⁴ C. Arnas, M. Mikikian, G. Bachet, and F. Doveil, Phys. Plasmas **7**, 4418 (2000).

- ³⁵ Dj. Bošan, V. Zlatić, and B. Mijović, *J. Phys. D: Appl. Phys.* **21**, 1462 (1988).
- ³⁶ C. Lotze, M. Corso, K. Franke, F. von Oppen, and J. Pascual, *Science* **338**, 779 (2012).
- ³⁷ J. Gupta, C. Lutz, A. Heinrich, and D. Eigler, *Phys. Rev. B* **71**, 115416 (2005).
- ³⁸ A. Senftleben, O. Al-Hagan, T. Pflüger, X. Ren, D. Madison, A. Dorn, and J. Ullrich, *J. Chem. Phys.* **133**, 044302 (2010).
- ³⁹ C. Arnas, M. Mikikian, and F. Doveil, *Phys. Rev. E* **60**, 7420 (1999).
- ⁴⁰ V. Fortov, A. Khrapak, S. Khrapak, V. Molotkov, and O. Petrov, *Phys. Usp.* **47**(5), 447 (2004).
- ⁴¹ A. Melzer, T. Trottenberg, and A. Piel, *Phys. Lett. A* **191**, 301 (1994).
- ⁴² N. Zouache and A. Lefort, *IEEE Trans. Dielectr. Electr. Insul.* **4**(4), 358 (1997).